Organic & Biomolecular Chemistry

Cite this: *Org. Biomol. Chem.*, 2011, **9**, 6034

www.rsc.org/obc

PAPER

Computational investigation on the mechanism and stereochemistry of guanidine-catalyzed enantioselective isomerization of 3-alkynoates to allenoates†

Dongfeng Huang, Song Qin* and Changwei Hu*

Received 22nd December 2010, Accepted 14th April 2011
DOI: 10.1039/c0ob01233e

The mechanism of guanidine-catalyzed enantioselective isomerization of 3-alkynoates to allenoates is investigated using density functional theory methods. The calculations predict that the isomerization reaction includes two hydrogen-transfer steps and one conformational change mediated by the TBO catalyst. The first hydrogen-transfer step corresponds to the migration of hydrogen from C_4 of the substrate to the guanidine catalyst, and the second one to the transfer of this hydrogen from the guanidine catalyst to C_6 of the substrate forming the product. The calculations predict that the first hydrogen-transfer step (deprotonation of the substrate) might be the rate-determining step for the overall reaction. In the chiral system, the evolution of IM1s is crucial for the enantioselectivity of the reaction, which is more relevant to the second hydrogen-transfer step *via* TS2. In TS2, the N–H $\cdots$ O hydrogen bond between the guanidine catalyst and the substrate, sensitive to the chiral environment, might account for the enantioselectivity of the isomerization reaction. The larger size of the substituted group at the chiral site of guanidine could selectively make one of the competing transition states unstable in terms of significantly decreasing the strength of the N–H $\cdots$ O hydrogen bond in the disfavored TS, which results in a high ee value.

1. Introduction

Allenes are present in many natural products, and their rich structural and reactive properties also render them uniquely versatile synthetic intermediates in organic synthesis.[1] New methods for the synthesis of allenes reflect their growing value and make them more attractive.[2] In experiments, most of the reported procedures are catalyzed or mediated by transition metal compounds, particularly by palladium, iron, copper *etc*.[3] However, metal catalysts often suffer from some apparent drawbacks, including the high cost of the catalysts, the use of noxious metals, the difficulty in separation of the product and the rigorous operation conditions.

On the other hand, the use of a wide range of small molecules as catalysts has emerged as an essential tool for asymmetric organic synthesis. A variety of key carbon–carbon and carbon–heteroatom bond-forming organic reactions has been realized under catalysis by small organic molecules, including organic acids and Lewis bases, *etc.*, leading to high yields and high enantioselectivities under mild conditions.[4]

For its strong Brønsted basicity and specific pattern of hydrogen bonding, guanidine has been successfully used as an efficient organocatalyst in the Henry reaction,[5] Michael addition,[6] Diels–Alder addition,[7] and other kinds of highly enantioselective reactions.[8] Recently, Tan's group reported that bicyclic guanidine A (Scheme 1) could catalyze the enantioselective isomerization of 3-alkynoates to chiral allenoates.[9] Their work developed a newly metal free entry to allene synthesis.

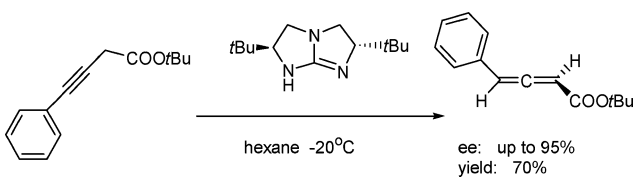

Scheme 1 Guanidine-catalyzed isomerization of 3-alkynoates.

However, much less is known about the mechanism of guanidine-catalyzed reaction based on quantum-chemistry. Han and co-workers investigated the mechanism of bicyclic guanidine-catalyzed Strecker reaction, and proposed that the guanidine was active in a double proton-transfer reaction.[10] Subsequent theoretical studies on the mechanism of triazabicyclodecene (TBD)-catalyzed ring-opening polymerization (ROP) of cyclic esters indicated that the polymerization reaction could proceed *via* a hydrogen bond mediated mechanism or an acetyl transfer mechanism, but the latter had a considerably higher barrier than the hydrogen bond-mediated mechanism.[11,12] Waymouth and coworkers put forward a nucleophilic mechanism where

Key Laboratory of Green Chemistry and Technology, Ministry of Education, College of Chemistry, Sichuan University, Chengdu, Sichuan, 610064, China. E-mail: qinsong@scu.edu.cn, gchem@scu.edu.cn

† Electronic supplementary information (ESI) available: Computational methods, energies, optimized geometries. See DOI: 10.1039/c0ob01233e

TBD reacted reversibly with esters to generate an acyl-TBD intermediate followed by a yield of amides.[13]

For the guanidine-catalyzed isomerization of 3-alkynoates, there is no detailed theoretical investigation available aiming at the mechanism and stereochemistry at the molecular level. In order to gain a better understanding of the guanidine-catalyzed isomerization of 3-alkynoates and provide useful clues to related guanidine-catalyzed asymmetric synthesis, theoretical investigations on the detailed mechanism have been performed using density functional theory (DFT) in the present work. The main purposes of this work are to identify the role of the bicyclic guanidine, and understand the detailed mechanism as well as the origin of the stereochemistry.

2. Computational details

To reduce the computational cost, the reaction mechanism of the guanidine-catalyzed isomerization of 3-alkynoate was investigated firstly using the model reaction system (Scheme 2). In this model system, a simplified non-chiral species ($R_1 = H$) was constructed as the model catalyst, and the R_2 group of the substrate was replaced by a methyl group. This approach is expected to provide detailed information about the properties of the reaction and give clues for further investigation on a real reaction system.

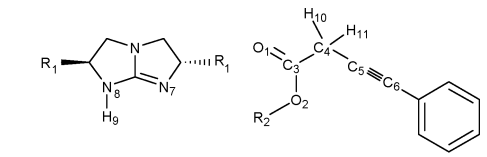

Scheme 2 Model reaction system used in the investigation of the mechanism of the guanidine-catalyzed isomerization of 3-alkynoate.

On the basis of the results from the model system, the aim of the present investigation turns to the reaction mechanism and the stereochemistry of the reaction using the actual molecules in terms of locating possible intermediates (IM) and transition states (TS). The actual chiral triazabicyclooctene (TBO) catalyst system, where $R_1 = R_2 = t$Bu, is constructed according to the literature, which has been experimentally proven to be an excellent enantioselective synthesis reaction with high yield and ee value.[9]

All calculations were performed with the Gaussian 03 programs.[14] The geometrical optimizations of all the intermediates and transition states were performed in the gas-phase with B3LYP functional[15] and 6-31+G(d,p) basis sets.[16] Frequencies were also calculated at the same level to confirm each stationary point to be either a minimum (no imaginary frequency) or a saddle point (unique imaginary frequency), and to obtain the zero-point correction. To evaluate the sensitivities of the calculations to basis sets, the reoptimization on the species along the most energy-favored in the model system (*cis*-path) was performed at the B3LYP/6-311++G(d,p)[16] level in the gas-phase. The discrepancies in geometries and relative energies of the corresponding structures calculated at the two levels were very small, suggesting that the present results were reasonable (see the ESI†). For each optimized structure, solvent effects were considered at the B3LYP/6-31+G(d,p) level using a self-consistent reaction field (SCRF) method based on the polarizable continuum model (PCM).[17] Because hexane was not available as solvent in the Gaussian 03 programs, we selected heptane as the solvent and use the dielectric constant (ε) of 1.904 in present calculations. Unless otherwise stated, the energy data used in the discussion are the total electronic energies in the PCM calculations corrected by the Gibbs energy correction in the gas-phase. The chemical bonding properties were analyzed following the concepts developed in the theory of atoms-in-molecules (AIM).[18] To obtain a further insight into the electronic properties, natural bond orbital (NBO)[19] analysis at the B3LYP/6-31+G(d,p) level was also performed.

Since the actual system is more comparable to the corresponding experiments, unless otherwise stated, the data from the actual system are presented in the following discussion. As preliminary results, the data from the simple model system are listed in the supporting information.†

3. Results and discussion

3.1 Mechanism of the guanidine-catalyzed isomerization of 3-alkynoate

Substrate–catalyst complex. The predicted reaction starts from the coordination of the substrate to the guanidine catalyst TBO. As shown in Fig. 1, the substrate has two conformations: the carbonyl oxygen of the substrate can alternatively be *cis* or *trans* to the alkyne. Because the *t*Bu group (R_2) of the substrate can be located *anti* or *syn* with respect to the adjacent *t*Bu (R_1) of the chiral catalyst, four distinct substrate–catalyst complexes are obtained, named as *anti-cis*-, *anti-trans*-, *syn-cis*- and *syn-trans*-COM, respectively. In these four complexes, the carbonyl oxygen of the substrate coordinates to the –NH of TBO with an H–O distance of about 2.0 Å, and the N–H $\cdots$ O moiety keeps a linear

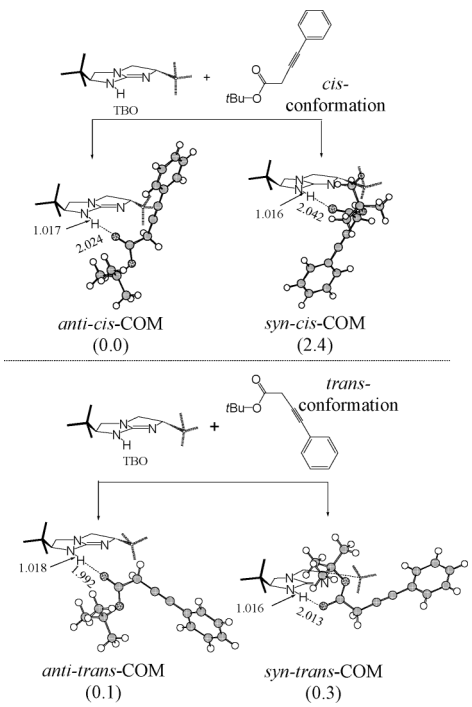

Fig. 1 Optimized structures of substrate–catalyst complexes; the relative Gibbs free energies (in kJ mol^{-1}) with respect to *anti-cis*-COM are listed in parentheses.

geometry. This means that there exists an N–H···O hydrogen bond between the carbonyl of the substrate and the Brønsted base catalyst TBO in each COM. The N–H···O hydrogen bond is also suggested by the Laplacian values at the critical point between $H_9 \cdots O_1$ from AIM analysis, which is *ca.* –0.015 au in these complexes. PCM calculations predict that these complexes might be nearly equally formed, as the largest difference in Gibbs free energy among them is no more than 2.4 kJ mol^{-1}.

Reaction paths. The reaction can take place from each substrate–catalyst complex, and therefore four reaction paths are available in the system. Here, the *anti-cis*-path from *anti-cis*-COM is chosen to illustrate the reaction mechanism. This path and the corresponding optimized structures are given in Fig. 2. The PESs of the entire reaction are plotted in Fig. 3.

From *anti-cis*-COM, the hydrogen atom (H_{11}) of the substrate transfers to TBO *via* an eight-membered ring transition state *anti-cis*-TS1 to generate the intermediate *anti-cis*-IM1 with an energy barrier of 52.0 kJ mol^{-1}. For *anti-cis*-TS1, the C_4–H_{11} bond points to TBO is stretched to 1.465 Å, while the N_7–H_{11} distance shortens to 1.260 Å, indicating that C_4–H_{11} bond is weakened and the N_7–H_{11} bond is partially formed. After this step, the C_4–H_{11} distance elongates to 2.011 Å in *anti-cis*-IM1, which suggests that the C_4–H_{11} bond is broken and the hydrogen atom (H_{11}) of the substrate transfers to TBO. The NBO charge of 0.853 *e* accumulated on the TBO–H moiety suggests that *anti-cis*-IM1 has a zwitterionic character.

In this deprotonation process, the N–H···O hydrogen bond is strengthened gradually, for its length decreases from 2.024 Å in *anti-cis*-COM to 1.568 Å in *anti-cis*-IM1 *via* 1.833 Å in *anti-cis*-TS1. The strengthened hydrogen bond in this reaction step is also supported by the Laplacian values at the critical point between $H_9 \cdots O_1$ from AIM analysis, which are –0.015 au in *anti-cis*-COM, –0.040 au in *anti-cis*-IM1 and –0.024 au in *anti-cis*-TS1, respectively.

Next, a conformational change occurs from *anti-cis*-IM1 *via* *anti-cis*-TSR, in which the guanidine moiety rotates around N–H···O hydrogen bond for the transferred hydrogen atom (H_{11}) to be ready to migrate to the C_6 atom of the substrate, leading to the formation of *anti-cis*-IM2. The intermediate *anti-cis*-IM2 also

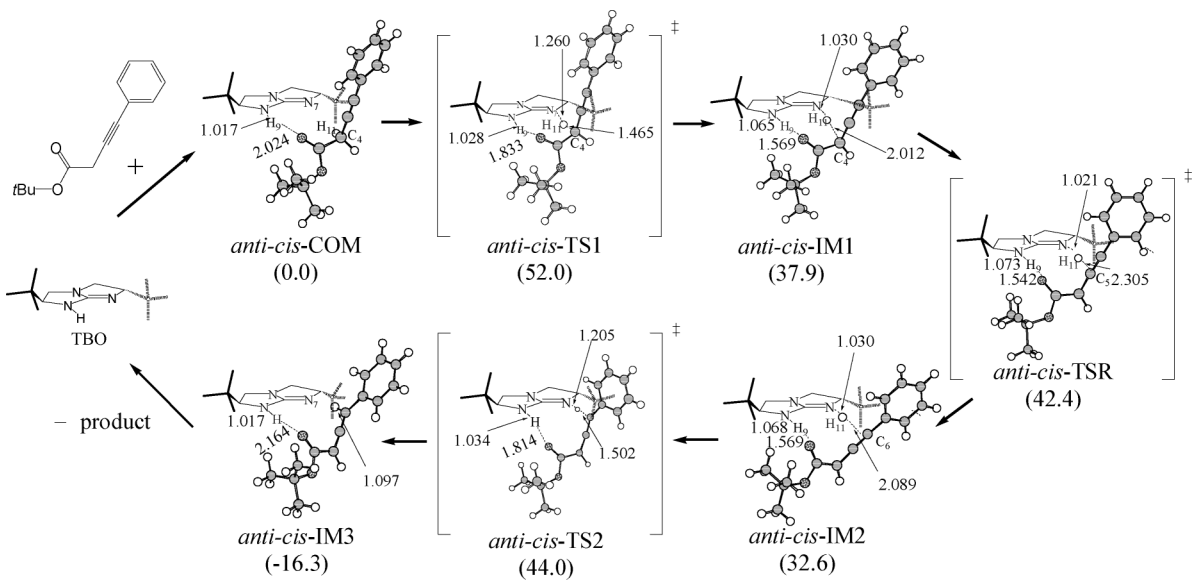

Fig. 2 Predicted reaction mechanism of the actual system. The bond lengths are in ångstroms and the relative Gibbs free energies (in kJ mol^{-1}) are listed in parentheses.

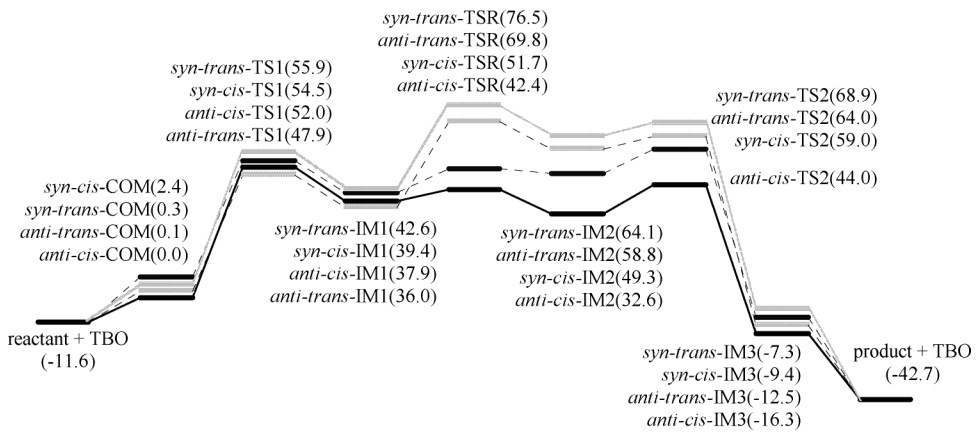

Fig. 3 Potential energy profile calculated at the B3LYP/6-31+G(d,p) level. The relative Gibbs free energies (in kJ mol^{-1}) are listed in parentheses.

possesses zwitterionic character, from the NBO charge of 0.855 *e* accumulated on the TBO–H moiety. In *anti-cis*-IM2, the N–H···O hydrogen bond between the carbonyl and TBO is slightly strengthened to 1.569 Å from 1.568 Å in *anti-cis*-IM1. PCM calculations show the Gibbs energy barrier of this step to be 4.5 kJ mol^{-1}. With such a smaller rotation barrier, the conformational change from *anti-cis*-IM1 to *anti-cis*-IM2 might be fast and take place easily. Similar conformational changes are also involved in the reaction mechanism of the TBD-catalyzed ROP proposed by Rice *et al.*[11]

Then, *anti-cis*-IM2 evolves to the product–complex *anti-cis*-IM3 *via* a ten-membered ring transition state *anti-cis*-TS2 with a low energy barrier of 11.4 kJ mol^{-1}. In this step, the H_{11} atom of TBO moves gradually to the C_6 atom, indicated by the corresponding C_6–H_{11} distance decreasing from 2.089 Å in *anti-cis*-IM2 to 1.097 Å in *anti-cis*-IM3 *via* 1.503 Å in *anti-cis*-TS2, meaning that the N–H···O hydrogen bond is gradually weakened. This is also confirmed by the AIM results. For *anti-cis*-TS2, the Laplacian value at the critical point between $H_9 \cdots O_1$ is –0.025 au, and for *anti-cis*-IM3, it becomes –0.012 au. As a result, after this step TBO returns the hydrogen atom (H_{11}) to the substrate with the formation of the product. Finally, the product is released from *anti-cis*-IM3 as the N–H···O hydrogen bond is broken with the recovery of TBO.

In summary, the calculations predict that the isomerization reaction includes two hydrogen-transfer steps and one conformational change mediated by the TBO catalyst. For all paths, the first hydrogen-transfer step corresponds to the migration of H_{11} from C_4 of the substrate to the TBO catalyst, and the second one to the transfer of this hydrogen from the TBO catalyst to C_6 of the substrate with the formation of the final product. For the *anti-cis*-path and the *syn-cis*-path, the conformational change corresponds to the rotation about the axis of the N–H···O hydrogen bond, while for the *anti-trans*-path and the *syn-trans*-path, this conformational change corresponds to the movement of the substrate with respect to TBO.

As the major part of the *anti-cis*-path represents the lowest energy curve in terms of Gibbs free energies, this path might be the most energy-favored in this chiral system. Furthermore, as shown in Fig. 3, as the first hydrogen-transfer step (deprotonation of the substrate) possesses the largest energy barrier, it might be the rate-determining step (RDS) for the overall reaction.

3.2 Stereochemistry of guanidine-catalyzed isomerization of 3-alkynoate

As shown in Fig. 3, although the RDS for the evolution of the reactants to the products is the first deprotonation step, the differences in energies for the deprotonation along four paths are very small, which means that all IM1s will be nearly equally formed.

According to the Curtin–Hammett principle,[20] the distribution of final products is not solely dependent on the relative proportions of IM1; it is also controlled by the difference in standard Gibbs energies of the respective TSs. For the *anti-trans*-path or the *syn-trans*-path, as the forward conformational change barrier (IM1 → TSR, *ca.* 33 kJ mol^{-1}) is much larger than the reverse energy barrier of the first deprotonation step (IM1 → TS1, *ca.* 13 kJ mol^{-1}), the first step might be reversible and the evolution of *trans*-IM1s to the final products might be remarkably hindered in the conformational change step. Besides, the energy curves along the *anti-trans* and *syn-trans*-path from IM1s stand much higher than the other two paths, which means that the evolution of IM1 along the *anti-trans*-path or *syn-trans*-path might be significantly inferior.

Along *anti-cis*-path or *syn-cis*-path, the rotation process possesses a very flat energy curve, meaning that *cis*-IM1 could evolve to *cis*-IM2 rapidly *via cis*-TSR. For the *anti-cis*-path, the remaining barriers for the evolution of *anti-cis*-IM1 to the final product are considerably smaller than the reverse energy barrier of the first step (*anti-cis*-IM1 → *anti-cis*-TS1, 14.1 kJ mol^{-1}). This implies that once *anti-cis*-IM1 forms, it could evolve to the product in *S*-configuration. In contrast, along the *syn-cis*-path, however, the energy barrier of *syn-cis*-IM1 → *syn-cis*-TS2 (19.6 kJ mol^{-1}) is larger than the reverse energy barrier of the first step (*syn-cis*-IM1 → *syn-cis*-TS1, 15.1 kJ mol^{-1}). As a result, the first step might be reversible and the evolution of *syn-cis*-IM1 might be relatively hindered at *syn-cis*-TS2. For these two paths, TS2 plays a role to facilitate or hinder the evolution of IM1 into products. Therefore, although the enantioselectivity of such a reaction involves multiple steps, the evolution of IM1s is crucial, which is more relevant to the second hydrogen-transfer step *via* TS2.

As shown in Fig. 4, for *anti-cis*-TS2 and *syn-cis*-TS2, the clear difference is the location of the *t*Bu of the substrate. In *syn-cis*-TS2, the *t*Bu of the substrate is located on the same side as the *t*Bu group of the catalyst, meaning that *syn-cis*-TS2 suffers more steric hindrance than its analogue *anti-cis*-TS2 in which the *t*Bu of the substrate lies on the opposite side to the *t*Bu group of the catalyst. This stronger steric hindrance makes *syn-cis*-TS2 looser and less stable than *anti-cis*-TS2, as suggested by the longer N–H···O hydrogen bond length (1.987 *vs.* 1.814 Å) and the relatively positive Laplacian value (–0.016 *vs.* –0.025 au) between the –NH and the carbonyl oxygen of the substrate. This means that this N–H···O hydrogen bond might be sensitive to the chiral environment and therefore make the competing transition states different from each other in relative energies. The calculations place *anti-cis*-TS2 15.0 kJ mol^{-1} lower than *syn-cis*-TS2 in terms of Gibbs free energies, corresponding to ee >99%. Because the *S*-configuration product is yielded *via anti-cis*-TS2, the *S*-product would be the predominant product with high ee value in the title isomerization reaction, which is in agreement with the experimental observation (*S*-product with 95% ee).[9]

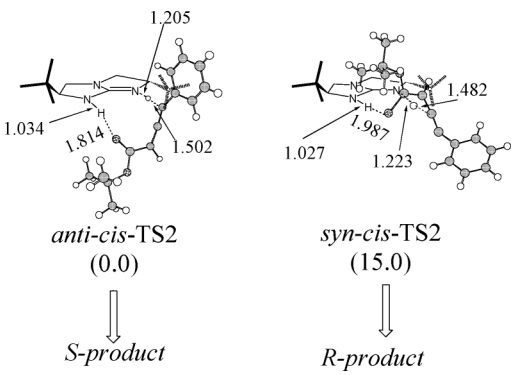

Fig. 4 Structures and the relative energies of the competing transition states (TS2s) in the actual system (in kJ mol^{-1}).

3.3 Origin of enantioselectivity

Next, the focus of the present investigation turns to the origin of the stereochemistry of the titled isomerization reaction and the influence of R_1 group of guanidine catalyst on it. Here, we used three substituents (Me, Et and *i*Pr) different in size to replace the *t*Bu at chiral sites in the actual system. The two competing transition states and the relative energies are shown in Fig. 5.

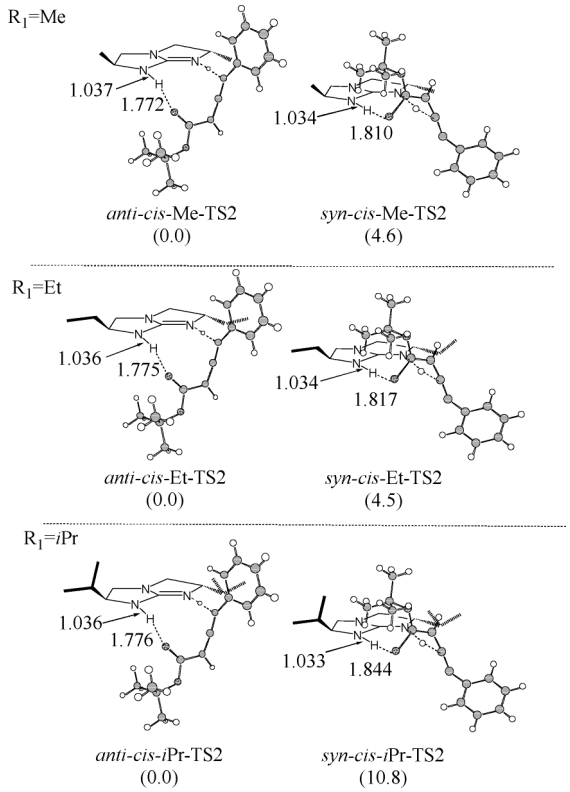

Fig. 5 Structures and relative energies of the competing transition state TS2s with different R_1 groups (in kJ mol^{-1}).

As shown in Fig. 5, it could be found that there exists an N–H $\cdots$ O hydrogen bond between the carbonyl of the substrate and the TBO catalyst in all TS2s. For all *anti-cis*-TS2s, the strength of the N–H $\cdots$ O hydrogen bond might not be sensitive to the R_1 groups, suggested by the fact that the length of the N–H $\cdots$ O hydrogen bond just slightly fluctuates around 1.8 Å with different R_1 groups. Therefore, it might be deduced that the size of the R_1 group does not exert a significant effect on the N–H $\cdots$ O hydrogen bond, when the *t*Bu of the substrate is *anti* to the adjacent R_1 group in *anti-cis*-TS2s. In contrast, if the *t*Bu is located *syn* to the R_1 group in *syn-cis*-TS2s, the length of the N–H $\cdots$ O hydrogen bond is drastically increased from 1.810 to 1.987 Å when the R_1 group changes from Me to *t*Bu. This means that the N–H $\cdots$ O hydrogen bond is remarkably weakened when R_1 groups become larger in the energy-disfavored transition states *syn-cis*-TS2s, which is also reflected by the corresponding Laplacian values (see Table 1). The above results further confirmed that the N–H $\cdots$ O hydrogen bond is sensitive to the chiral environment, and in particular to the size of the R_1 group. On the other hand, the energy gap (ΔG) between *anti-cis*-TS2 and *syn-cis*-TS2 (R_1 = Me, Et, *i*Pr and *t*Bu) is 4.6, 4.5, 10.8 and 15.0 kJ mol^{-1}, respectively, indicating that the larger R_1 groups result in greater ΔG in general. It is supposed that the R_1 groups might weaken the N–H $\cdots$ O hydrogen bond in energy-disfavored transition states and increase ΔG between the competing transition states, which might be the origin of the enantioselectivity of the title isomerization reaction.

Moreover, the difference in the N–H $\cdots$ O hydrogen bond lengths between *anti-cis*-TS2 and *syn-cis*-TS2, defined as Δr, are 0.038, 0.042, 0.068, 0.173 Å when R_1 = Me, Et, *i*Pr and *t*Bu, respectively. Combined with ΔG between *anti-cis*-TS2s and *syn-cis*-TS2s, it can be found that there might be an apparent positive relationship between Δr and ee value (see Table 1). Although the N–H $\cdots$ O hydrogen bond should not be the unique factor to determine the energies of TS2s, Δr can be regarded as a vital geometrical parameter associated with the stereochemistry.

To sum up, the enantioselectivity should be controlled by the N–H $\cdots$ O hydrogen bond between –NH of the guanidine catalyst and the carbonyl oxygen of the substrate. When larger R_1 groups exist at the chiral sites of the catalyst, they could selectively make one of the competing transition states unstable in terms of decreasing the strength of this N–H $\cdots$ O hydrogen bond in the disfavored one. In the present case, the *S*-configuration catalyst makes *syn-cis*-TS2 unstable due to the steric hindrance between the R_1 group and the *t*Bu group of the substrate, and therefore leads to the predominant *S*-product. Moreover, it is also found that the ee value is significantly dependent on the size of the R_1 groups: when larger R_1 groups are introduced (such as *t*Bu) at the chiral sites of guanidine, ΔG between two competing transition states becomes great enough for high ee values.

4. Conclusions

The major conclusions are listed as follows:

1. The title isomerization reaction includes two hydrogen-transfer steps and one conformational change mediated by the TBO catalyst. The first hydrogen-transfer step corresponds to the migration of hydrogen from C_4 of the substrate to the guanidine catalyst, and the second one to the transfer of this hydrogen from the guanidine catalyst to C_6 of the substrate forming the product. The calculations predict that the first hydrogen-transfer

Table 1 Relationship between Δr and ΔG value

R_1	$r_{O\text{-}H}$ in *anti-cis*-TS2 (Å)	$r_{O\text{-}H}'$ in *syn-cis*-TS2 (Å)	Δr (Å)	ΔG (kJ mol^{-1})
Me	1.772 (–0.027)[a]	1.810 (–0.025)	0.038	4.6
Et	1.775 (–0.027)	1.817 (–0.024)	0.042	4.5
*i*Pr	1.776 (–0.027)	1.844 (–0.024)	0.068	10.8
*t*Bu	1.814 (–0.025)	1.987 (–0.016)	0.173	15.0

[a] Corresponding Laplacian values (in au).

step (deprotonation of the substrate) to IM1s might be the rate-determining step for the overall reaction.

2. The N–H · · · O hydrogen bond between –NH of the guanidine catalyst and the carbonyl oxygen of the substrate, sensitive to the chiral environment, might account for the enantioselectivity. The larger size of the substituent group at the chiral site of guanidine could selectively make one of the competing transition states unstable in terms of significantly decreasing the strength of the N–H · · · O hydrogen bond in the disfavored TS. This means that a larger R_1 group is necessary to achieve the desired ee value of such isomerization reactions.

Acknowledgements

The authors are grateful for financial support from the NNSFC (Nos. 20732003, 20772085 and 21021001), PCSIRT (No. IRT0846).

References

1 For reviews, see: (*a*) A. Hoffmann-Röder and N. Krause, *Angew. Chem., Int. Ed.*, 2004, **43**, 1196; (*b*) S. Ma, *Chem. Rev.*, 2005, **105**, 2829; (*c*) T. Bai, S. Ma and G. Jia. Coord, *Chem. Rev.*, 2009, **25**, 423.

2 For recent examples, see: (*a*) J. L. García Ruano, V. Marcos and J. Alemán, *Angew. Chem., Int. Ed.*, 2008, **47**, 6836; (*b*) H. Jiang, X. Liu and L. Zhou, *Chem.–Eur. J.*, 2008, **14**, 11305; (*c*) H. Zhang, X. Fu, J. Chen, E. Wang, Y. Liu and Y. Li, *J. Org. Chem.*, 2009, **74**, 9351; (*d*) R. V. Kolakowski, M. Manpadi, Y. Zhang, T. J Emge and L. J. Williams, *J. Am. Chem. Soc.*, 2009, **131**, 12910; (*e*) Z. J. Zheng, X. Z. Shu, K. G. Ji, S. C. Zhao and Y. M. Liang, *Org. Lett.*, 2009, **11**, 3214; (*f*) C. Deutsch, B. H. Lipshutz and N. Krause, *Org. Lett.*, 2009, **11**, 5010; (*g*) X. Zeng, G. D. Frey, S. Kousar and G. Bertrand, *Chem.–Eur. J.*, 2009, **15**, 3056; (*h*) X. Tang, S. Woodward and N. Krause, *Eur. J. Org. Chem.*, 2009, 2836; (*i*) D. R. Fandrick, J. T. Reeves, Z. Tan, H. Lee, J. J. Song, N. K. Yee and C. H. Senanayake, *Org. Lett.*, 2009, **11**, 5458; (*j*) P. Cérat, P. J. Gritsch, S. R. Goudreau and A. B. Charette, *Org. Lett.*, 2010, **12**, 564.

3 For reviews, see: (*a*) L. K. Sydnes, *Chem. Rev.*, 2003, **103**, 1133; (*b*) S. Ma, *Acc. Chem. Res.*, 2003, **36**, 701; (*c*) N. Krause and A. Hoffmann-Röder, *Tetrahedron*, 2004, **60**, 11671; (*d*) M. Ogasawara, *Tetrahedron: Asymmetry*, 2009, **20**, 259.

4 For reviews, see: (*a*) K. A. Schug and W. Lindner, *Chem. Rev.*, 2005, **105**, 67; (*b*) E. N. Jacobsen and M. S. Taylor, *Angew. Chem., Int. Ed.*, 2006, **45**, 1520; (*c*) A. G. Doyle and E. N. Jacobsen, *Chem. Rev.*, 2007, **107**, 5713; (*d*) E. A. C. Davie, S. M. Mennen, Y. Xu and S. J. Miller, *Chem. Rev.*, 2007, **107**, 5759; (*e*) A. Dondoni and A. Massi, *Angew. Chem., Int. Ed.*, 2008, **47**, 4638; (*f*) D. Leow and C. H. Tan, *Chem.–Asian J.*, 2009, **4**, 488.

5 (*a*) Y. Sohtome, Y. Hashimoto and K. Nagasawa, *Adv. Synth. Catal.*, 2005, **347**, 1643; (*b*) Y. Sohtome, Y. Hashimoto and K. Nagasawa, *Eur. J. Org. Chem.*, 2006, 2894; (*c*) Y. Sohtome, N. Takemura, T. Iguchi, Y. Hashimoto and K. Nagasawa, *Synlett*, 2006, **1**, 144; (*d*) K. Takadaa and K. Nagasawaa, *Adv. Synth. Catal.*, 2009, **351**, 345.

6 (*a*) T. Ishikawa, Y. Araki, T. Kumamoto, H. Seki, K. Fukuda and T. Isobe, *Chem. Commun.*, 2001, 245; (*b*) M. Terada, H. Ube and Y. Yaguchi, *J. Am. Chem. Soc.*, 2006, **128**, 1454; (*c*) X. Fu, Z. Jiang and C.-H. Tan, *Chem. Commun.*, 2007, 5058; (*d*) A. Ryoda, N. Yajima, T. Haga, T. Kumamoto, W. Nakanishi, M. Kawahata, K. Yamaguchi and T. Ishikawa, *J. Org. Chem.*, 2008, **73**, 133; (*e*) O. Mahé, D. Frath, I. Dez, F. Marsais, V. Levacher and J.-F. Brière, *Org. Biomol. Chem.*, 2009, **7**, 3648; (*f*) Z. Yu, X. Liu, L. Zhou, L. Lin and X. M. Feng, *Angew. Chem.*, 2009, **121**, 5297.

7 J. Shen, T. T. Nguyen, Y. P. Goh, W. P. Ye, X. Fu, J. Y. Xu and C. H. Tan, *J. Am. Chem. Soc.*, 2006, **128**, 13692.

8 For other examples, see: (*a*) E. J. Corey and M. J. Grogan, *Org. Lett.*, 1999, **1**, 157; (*b*) T. Kita, A. Georgieva, Y. Hashimoto, T. Nakata and K. Nagasawa, *Angew. Chem.*, 2002, **114**, 2956; (*c*) D. Basavaiah, K. V. Rao and B. S. Reddy, *Tetrahedron: Asymmetry*, 2006, **17**, 1036; (*d*) T. Kita, B. Shin, Y. Hashimoto and K. Nagasawa, *Heterocycles*, 2007, **73**, 241; (*e*) M. Terada, T. Ikehara and H. Ube, *J. Am. Chem. Soc.*, 2007, **129**, 14112; (*f*) C. Uyeda and E. N. Jacobsen, *J. Am. Chem. Soc.*, 2008, **130**, 9228; (*g*) S. Kobayashi, R. Yazaki, K. Seki and Y. Yamashita, *Angew. Chem., Int. Ed.*, 2008, **47**, 5613; (*h*) D. Leow, S. S. Lin, K. S. Chittimalla, X. Fu and C. H. Tan, *Angew. Chem., Int. Ed.*, 2008, **47**, 5641; (*i*) B. Shin, S. Tanaka, T. Kita, Y. Hashimoto and K. Nagasawa, *Heterocycles*, 2008, **76**, 801; (*j*) M. Terada, D. Tsushima and M. Nakanoa, *Adv. Synth. Catal.*, 2009, **351**, 2817; (*k*) Z. Y. Jiang, Y. Yang, Y. Pan, Y. Zhao, H. J. Liu and C. H. Tan, *Chem.–Eur. J.*, 2009, **15**, 4925; (*l*) Z. Y. Jiang, Y. Pan, Y. Zhao, T. Ma, R. Lee, Y. Yang, K. W. Huang, M. W. Wong and C. H. Tan, *Angew. Chem., Int. Ed.*, 2009, **48**, 3627.

9 H. J. Liu, D. Leow, K. W. Huang and C. H. Tan, *J. Am. Chem. Soc.*, 2009, **131**, 7212.

10 J. Li, W. Y. Jiang, K. L. Han, G. Z. He and C. Li, *J. Org. Chem.*, 2003, **68**, 8786.

11 A. Chuma, H. W. Horn, W. C. Swope, R. C. Pratt, L. Zhang, B. G. G. Lohmeijer, C. G. Wade, R. M. Waymouth, J. L. Hedrick and J. E. Rice, *J. Am. Chem. Soc.*, 2008, **130**, 6749.

12 L. Simón and J. M. Goodman, *J. Org. Chem.*, 2007, **72**, 9656.

13 M. K. Kiesewetter, M. D. Scholten, N. Kirn, R. L. Weber, J. L. Hedrick and R. M. Waymouth, *J. Org. Chem.*, 2009, **74**, 9490.

14 M. J. Frisch, G. W. Trucks, H. B. Schlegel, G. E. Scuseria, M. A. Robb, J. R. Cheeseman, J. A. Montgomery, Jr., T. Vreven, K. N. Kudin, J. C. Burant, J. M. Millam, S. S. Iyengar, J. Tomasi, V. Barone, B. Mennucci, M. Cossi, G. Scalmani, N. Rega, G. A. Petersson, H. Nakatsuji, M. Hada, M. Ehara, K. Toyota, R. Fukuda, J. Hasegawa, M. Ishida, T. Nakajima, Y. Honda, O. Kitao, H. Nakai, M. Klene, X. Li, J. E. Knox, H. P. Hratchian, J. B. Cross, V. Bakken, C. Adamo, J. Jaramillo, R. Gomperts, R. E. Stratmann, O. Yazyev, A. J. Austin, R. Cammi, C. Pomelli, J. Ochterski, P. Y. Ayala, K. Morokuma, G. A. Voth, P. Salvador, J. J. Dannenberg, V. G. Zakrzewski, S. Dapprich, A. D. Daniels, M. C. Strain, O. Farkas, D. K. Malick, A. D. Rabuck, K. Raghavachari, J. B. Foresman, J. V. Ortiz, Q. Cui, A. G. Baboul, S. Clifford, J. Cioslowski, B. B. Stefanov, G. Liu, A. Liashenko, P. Piskorz, I. Komaromi, R. L. Martin, D. J. Fox, T. Keith, M. A. Al-Laham, C. Y. Peng, A. Nanayakkara, M. Challacombe, P. M. W. Gill, B. G. Johnson, W. Chen, M. W. Wong, C. Gonzalez and J. A. Pople, *GAUSSIAN 03 (Revision B.05)*, Gaussian, Inc., Wallingford, CT, 2004.

15 A. D. Becke, *J. Chem. Phys.*, 1993, **104**, 5648.

16 (*a*) R. Ditchfield, W. J. Hehre and J. A. Pople, *J. Chem. Phys.*, 1971, **54**, 724; (*b*) W. J. Hehre, R. Ditchfield and J. A. Pople, *J. Chem. Phys.*, 1972, **56**, 2257; (*c*) P. C. Hariharan and J. A. Pople, *Mol. Phys.*, 1974, **27**, 209; (*d*) M. S. Gordon, *Chem. Phys. Lett.*, 1980, **76**, 163; (*e*) P. C. Hariharan and J. A. Pople, *Theor. Chim. Acta*, 1973, **28**, 213; (*f*) J. P. Blaudeau, M. P. McGrath, L. A. Curtiss and L. Radom, *J. Chem. Phys.*, 1997, **107**, 5016; (*g*) M. M. Francl, W. J. Pietro, W. J. Hehre, J. S. Binkley, D. J. DeFrees, J. A. Pople and M. S. Gordon, *J. Chem. Phys.*, 1982, **77**, 3654; (*h*) R. C. Binning Jr and L. A. Curtiss, *J. Comput. Chem.*, 1990, **11**, 1206; (*i*) V. A. Rassolov, J. A. Pople, M. A. Ratner and T. L. Windus, *J. Chem. Phys.*, 1998, **109**, 1223; (*j*) V. A. Rassolov, M. A. Ratner, J. A. Pople, P. C. Redfern and L. A. Curtiss, *J. Comput. Chem.*, 2001, **22**, 976.

17 (*a*) S. Miertus, E. Scrocco and J. Tomasi, *Chem. Phys.*, 1981, **55**, 117; (*b*) S. Miertus and J. Tomasi, *Chem. Phys.*, 1982, **65**, 239; (*c*) M. Cossi, V. Barone, R. Cammi and J. Tomasi, *Chem. Phys. Lett.*, 1996, **255**, 327; (*d*) M. Cossi, V. Barone, R. Cammi, B. Mennucci and J. Tomasi, *Chem. Phys. Lett.*, 1998, **286**, 253; (*e*) E. Cances, B. Mennucci and J. Tomasi, *J. Chem. Phys.*, 1997, **107**, 3032.

18 R. F. W. Bader, *Atoms in Molecules. A Quantum Theory*; Clarendon Press, Oxford, 1990. For computer programs, see: Biegler-König, F. W. Schönbohm, AIM2000. The program can be downloaded at http://www.aim2000.de/.

19 (*a*) J. Blaudeau, M. P. McGrath, L. A. Curtiss and L. Radom, *J. Chem. Phys.*, 1997, **107**, 5016; (*b*) M. M. Francl, W. J. Pietro, W. J. Hehre, J. S. Binkley, D. J. DeFrees, J. A. Pople and M. S. Gordon, *J. Chem. Phys.*, 1982, **77**, 3654.

20 (*a*) J. I. Seeman, *J. Chem. Educ.*, 1986, **63**, 42; (*b*) J. I. Seeman, *Chem. Rev.*, 1983, **83**, 84.